# Mass extinctions drove increased global faunal cosmopolitanism on the supercontinent Pangaea

Button, David; Lloyd, Graeme; Ezcurra, Martin; Butler, Richard

# Mass extinctions drove increased global faunal cosmopolitanism on the supercontinent Pangaea

David J. Button[1,2,3]*, Graeme T. Lloyd[4], Martín D. Ezcurra[1,5], and Richard J. Butler[1]*

[1]School of Geography, Earth and Environmental Sciences, University of Birmingham, Edgbaston, Birmingham, B15 2TT, United Kingdom.

[2]Current address: North Carolina Museum of Natural Sciences, Raleigh, NC 27607, USA; david.button44@gmail.com

[3]Current address: North Carolina State University, Department of Biological Sciences, 3510 Thomas Hall, Campus Box 7614, Raleigh, NC 27695, USA.

[4]School of Earth and Environment, Maths/Earth and Environment Building, The University of Leeds, Leeds, LS2 9JT, United Kingdom.

[5]Sección Paleontología de Vertebrados, CONICET−Museo Argentino de Ciencias Naturales "Bernardino Rivadavia", Avenida Ángel Gallardo 470, Buenos Aires, C1405DJR, Argentina.

Correspondence and requests for materials should be addressed to D.J.B. (email: david.button44@gmail.com) or R.J.B. (email: r.butler.1@bham.ac.uk).

**Editor's summary:** Mass extinctions are thought to produce 'disaster faunas', communities dominated by a small number of widespread species. Here, Button and colleagues develop a phylogenetic network approach to test this hypothesis and find that mass extinctions did increase faunal cosmopolitanism across the supercontinent Pangaea during the late Palaeozoic and early Mesozoic.

**Abstract:** Mass extinctions have profoundly impacted the evolution of life through not only reducing taxonomic diversity but also reshaping ecosystems and biogeographic patterns. In particular, they are considered to have driven increased biogeographic cosmopolitanism, but quantitative tests of this hypothesis are rare and have not explicitly incorporated information on evolutionary relationships. Here we quantify faunal cosmopolitanism using a phylogenetic network approach for 891 terrestrial vertebrate species spanning the late Permian through Early Jurassic. This key interval witnessed the Permian-Triassic and Triassic-Jurassic mass extinctions, the onset of fragmentation of the supercontinent Pangaea, and the origins of dinosaurs and many modern vertebrate groups. Our results recover significant increases in global faunal cosmopolitanism following both mass extinctions, driven mainly by new, widespread taxa, leading to homogenous "disaster faunas". Cosmopolitanism subsequently declines in post-recovery communities. These shared patterns in both biotic crises suggest that mass extinctions have predictable influences on animal distribution and may shed light on biodiversity loss in extant ecosystems.

Earth history has been punctuated by mass extinction events [1], biotic crises that fundamentally alter both biodiversity and biogeographic patterns [1,2]. A common generalisation is that mass extinctions are followed by periods of increased faunal cosmopolitanism [1–4]. For example, the Early Triassic aftermath of the Permian-Triassic mass extinction, the largest extinction event known [5,6], has been considered as characterized by a globally homogeneous 'disaster fauna' dominated by a small number of widely distributed and abundant taxa [1,3,6–8]. Similar patterns have been proposed for the aftermath of the mass extinction at the end of the Triassic [9]. However, explicit quantitative tests of changes in cosmopolitanism across mass extinctions are rare and have been limited to small geographical regions [3] or have not incorporated information from evolutionary relationships (phylogeny) [2,3].

In order to test the impact of mass extinctions on biogeographic patterns, a method for quantifying relative changes in cosmopolitanism through time is required. Sidor *et al*. [3] proposed that spatial occurrence data can be modelled as a bipartite taxon-locality network, specifying the distribution of fossil taxa (e.g., species) within defined localities (e.g., geographic areas such as continents or basins). The biogeographic structure of this network can then be quantified. Faunal heterogeneity (or biogeographic connectedness, BC) can be measured as the rescaled density of the network – the number of taxa actually shared between localities relative to the total possible number of taxon links between them[3] (Fig. 1a, b). Higher values of BC equate to increased cosmopolitanism (i.e., less heterogeneity), whereas decreases in BC indicate increasing faunal endemism or provinciality (i.e., greater heterogeneity). This approach has been previously applied to assess regional changes in cosmopolitanism within southern Gondwana across the Permian-Triassic mass extinction [3]. Results indicated a decline in BC from the late Permian to the Middle Triassic, indicating that cosmopolitanism increased following the extinction event. However, this study did not

include the critical immediate post-extinction faunas (earliest Triassic), and it is also unclear whether this regional signal is representative of global biogeographic trends.

This network method uses only binary presence-absence data – i.e., information on whether a given species was present (and sampled) within a given locality or not. It does not explicitly incorporate information on the supra-specific phylogenetic relationships between taxa, such as could be used to estimate phylogenetic distance present between different species present at different localities. As such, it may be difficult or impossible to apply to a global fossil record dominated by singletons (species occurring at just one locality), as is common for tetrapods. Moreover, the results are potentially sensitive to systematic variation in taxonomic practice (i.e., 'lumping' versus 'splitting') and differential temporal and spatial sampling. Consequently, it may be useful to consider how closely related sets of species from pairs of localities are on a continuous scale.

Here we present a modification of this network model that addresses these issues by incorporating phylogenetic information into the calculation of BC. Rather than treating links between taxa in different geographic regions in a binary fashion, they are instead inversely weighted in proportion to the phylogenetic distance between them (Fig. 1a, c). These reweighted links are then used to calculate phylogenetic biogeographic connectedness (pBC). As with BC, higher levels of pBC equate to more cosmopolitan faunas, with less phylogenetic distance between sets of species from pairs of localities. By contrast, lower values of pBC indicate greater endemism, and increased phylogenetic disparity between sets of species from pairs of localities. This method was applied using an informal supertree (figure 2a; Supplementary Note 1) and species-level occurrence dataset of terrestrial amniotes ranging from the late Permian to late Early Jurassic (c. 255–175 Ma; see Supplementary Note 2).A k-means cluster analysis was used to group taxa into ten distinct geographical regions based on their occurrence palaeocoordinates (figure 2b; Supplementary Information Note 3).

The sampled interval includes the Permian-Triassic and Triassic-Jurassic mass extinction events, and the origins of key terrestrial vertebrate clades such as crocodylomorphs, dinosaurs, lepidosaurs, mammaliaforms, pterosaurs, and turtles [9]. It is of particular biogeographic interest due to the presence of the supercontinent Pangaea [10], which began to break apart by the Early Jurassic. Although barriers to dispersal might be perceived as sparse on a supercontinent, numerous studies have suggested faunal provinciality and endemism on Pangaea, perhaps driven by climatic variation [3,9,11–13]. Our methodological approach allows patterns of global provincialism to be quantified, and the impact of mass extinctions on faunal cosmopolitanism tested, within an explicit phylogenetic context. Results demonstrate the evolution of relatively cosmopolitan 'disaster faunas' following both the Permian-Triassic and Triassic-Jurassic mass extinctions, suggesting that mass extinctions may have common biogeographical consequences.

## Results

**Global phylogenetic network biogeography results**. A marked and significant increase in global phylogenetic biogeographic connectedness (pBC) is observed across the Permian-Triassic mass extinction (Fig. 3). A gentle, non-significant, decrease occurs from the Early Triassic to the Middle Triassic. This is followed by a strong, significant decrease to minimum pBC values (and so maximum provincialism) in the Late Triassic. A significant increase in pBC is then observed after the Triassic-Jurassic mass extinction, in the early Early Jurassic, although pBC does not reach the levels seen in the Early Triassic. Phylogenetic BC declines to levels similar to those seen in the Late Triassic by the end of the Early Jurassic. These results show no correlation with the number of taxa or regions sampled in each time bin

(Supplementary Note 4, Supplementary Figs 1, 2, 3)and appear robust to variance in time bin length (Supplementary Figs 3d, 4).

Results for non-phylogenetic network biogeographic connectedness (non-phylogenetic BC) of the global dataset significantly differ from the phylogenetic results (Fig. 3). An overall decline in non-phylogenetic BC is still observed through the Triassic, but differences between the Lopingian, Early Triassic, and Middle Triassic time bins are not significant. In addition, no increase in non-phylogenetic BC is observed over the Triassic-Jurassic boundary.

**Global analysis of taxon subsets**. An increase in global pBC across a mass extinction boundary may result from preferential survivorship of cosmopolitan lineages [8,14–17], radiation of opportunistic 'disaster taxa' [6], or both. In order to test which of these processes drove observed increases in global pBC, we carried out additional analyses on subsets of our data. The first set of comparisons was restricted to those less inclusive clades that exhibit high levels of survivorship across each extinction event, thereby removing the influence of preferential extinction and focusing on patterns for clades established prior to the extinction. Among these taxa, a significant change in pBC is no longer observed across the Permian-Triassic boundary (Fig. 4a), although the increase across the Triassic-Jurassic mass extinction remains significant (Fig. 4b). The second set of comparisons focused on novel, recently-diverging clades, and demonstrates very high levels of pBC for these taxa in both the Early Triassic and the earliest Jurassic, significantly greater than total pBC in both these and the preceding time bins (Fig. 4a, b). Comparison of recently diverging clades in all time bins recovers the same signal as that from the total dataset (Supplementary Note 5, Supplementary Fig. 5), indicating that variation in pBC is not a result of differences in average clade age in each time bin.

**Geographically localised analyses**. To compare hemispherical trends in biogeographic connectedness, pBC was also calculated for Laurasia and Gondwana separately. The signal from Laurasian occurrences matches very closely with the global pattern (Fig. 5a). By contrast, patterns in Gondwana diverge markedly from global trends in the latest Triassic, where pBC abruptly rises, and then gradually declines through the Early Jurassic (Fig. 5a).

In addition, pBC analysis was implemented on terrestrial amniote occurrences from the southern Gondwanan dataset of Sidor *et al*. [3]. This dataset groups taxa at a geological basin, rather than broader regional, level; as a consequence, this analysis indicates how pBC differs at geographically smaller scales. Biogeographic connectedness is lower in the Middle Triassic than in the late Permian under both phylogenetic and non-phylogenetic treatments of these data (Fig. 5b); however, the result is not significant for phylogenetic BC.

## Discussion

The Triassic represents an important time in the evolution of vertebrate life on land. It witnessed a series of turnover events that resulted in a major faunal transition from Palaeozoic communities, dominated by non-mammalian synapsids and parareptiles, to more modern faunas including clades such as crocodylomorphs, dinosaurs, lepidosaurs, mammaliaforms , and turtles [9,18]. Our novel phylogenetic network approach helps to place these major faunal transitions of the Triassic within a global biogeographical context by allowing changes in faunal connectivity to be quantified within an explicit evolutionary framework.

Our results demonstrate an overall decrease in pBC from the Lopingian to the Early Jurassic, but punctuated by significant increases across both the Permian-Triassic and Triassic-Jurassic mass extinction events. This provides quantitative support for classically held hypotheses about the presence of a global cosmopolitan fauna in the aftermath of and in

response to these events [2,3]. The robustness of these results to sampling variation and variable time bin length supports their interpretation as real biogeographical signals.

Our taxon subset analyses were explicitly aimed at disentangling the impact of alternative mechanisms that could lead to this pattern of increased post-extinction pBC. Novel clades, those diverging immediately prior to or immediately after each mass extinction, were analysed separately and exhibit relatively high levels of pBC (i.e., increased cosmopolitanism relative to the preceding time bin) in both the Early Triassic and earliest Jurassic (Fig. 4a, b). By contrast, surviving clades, those well-established prior to the extinction and extending through it, exhibit no increase across the Permian-Triassic boundary and only a moderate increase across the Triassic-Jurassic boundary (Fig. 4b). This indicates that the increases in pBC following each extinction were primarily driven by the opportunistic radiation of novel taxa to generate cosmopolitan 'disaster faunas', rather than being due to preferential extinction of endemic taxa [19]. Recently-diverging clades in other time bins do not exhibit elevated pBC (Supplementary Note 5) and there is no correlation between pBC and average branch length in each time bin (Supplementary Note 6, Supplementary Fig. 6), indicating that this result is due to abnormal conditions following each mass extinction as opposed to being a property of clade age.

The global biogeographic restructuring of biological communities associated with these mass extinction events hence provides evidence of the release of biotic constraints [3], which would have facilitated the radiation of new or previously marginal groups, such as archosaurs following the Permian-Triassic mass extinction [3], and dinosaurs and mammaliaforms during the Early Jurassic [20,21]. This highlights the importance of historical contingency in the history of life, where unique events such as mass extinctions have exerted strong influences on the subsequent macroevolutionary patterns observed in deep time [22–24].

183 The global pBC pattern recovered here differs from the more geographically focused
184 and temporally limited non-phylogenetic study of Sidor *et al*. [3], which found Middle Triassic
185 levels of BC in southern Pangaea to be lower than those seen in the late Permian. Reanalysis
186 of the amniote occurrences from the basin-level dataset of Sidor *et al*. demonstrates that pBC
187 also declines between these time bins, although not significantly (Fig. 5b). Looking more
188 broadly, pBC trends in Gondwana differ from those seen in Laurasia (Fig. 5a). This is
189 particularly evident in the Late Triassic and Early Jurassic, in which a significant increase
190 and decrease in pBC is seen in Laurasia for each time bin, respectively, but not in Gondwana
191 (Fig. 5a).

192 These results suggest that localised biogeographic patterns within Gondwana may
193 have been decoupled from those seen elsewhere in the northern hemisphere. This would
194 corroborate previous work suggesting the evolution of a distinct fauna, that includes
195 massopodan sauropodomorphs, ornithischians, basal saurischians, and prozostrodontian
196 cynodonts as relatively common taxa in South America and Africa during the Late Triassic
197 [11]. The occurrences of guaibasaurids [25] and floral similarities [26,27] provide some links between
198 South American communities and the upper Maleri Formation of India, although the latter
199 assemblage remains relatively poorly-known and sampled. The Triassic-Jurassic mass
200 extinction was a global event [19] and it is unclear why decoupling of biogeographic trends
201 within Gondwana should occur. Sampling within Gondwana during this interval is uneven,
202 with the bulk of occurrences coming from palaeolatitudes between 30-60°S (see
203 Supplementary Note 4). During the Late Triassic the 30-60° latitudinal belts were dominated
204 by subtropical desert [28]. Interestingly, whereas this biome was more fragmented by seasonally
205 wet conditions through into the Jurassic within Laurasia, it remained relatively stable in
206 Gondwana [26,28]. It is possible that this stability may have contributed to the evolution of a
207 distinct fauna in the southern hemisphere. Alternatively, however, this distinct Gondwanan

pattern may be a sampling artefact. Although the inclusion of phylogenetic information allows the approach used here to incorporate more data than previous methods, sampling of latest Triassic and earliest Jurassic Gondwanan localities is relatively poor and uneven, leading to the low statistical power of results within these time bins. In the earliest Jurassic, in particular, over 80% of Gondwanan tetrapod occurrences are from the upper Elliot and Clarens formations of South Africa. Further evaluation of this possible signal will require sampling of new Late Triassic and Early Jurassic Gondwanan localities, particularly from India and Antarctica.

Under our non-phylogenetic network analysis of the global dataset, no increase in BC is observed across the Triassic-Jurassic boundary; indeed, no significant differences are observed between any consecutive time bins (Fig. 3). This highlights the importance of including phylogenetic information in global analyses such as that conducted here; without the incorporation of phylogeny, aspects of biogeographic signal may be obscured. The decline of pBC to minimal levels towards the end of the Triassic supports hypotheses of strong faunal provinciality and increased endemism within Pangaea during the early Mesozoic [3,9,12,13,29]. The distribution of Late Triassic tetrapods varies with latitude [9,11–13], a pattern also observed in terrestrial floras [9,27]. This is somewhat unexpected, given that oceanic barriers to dispersal were scant [30] and the latitudinal temperature gradient was weak [28] in Pangaea during the Late Triassic. Instead, the 'mega-monsoonal' climate of Late Triassic Pangaea [28] would have driven provinciality of faunas through strong latitudinal and seasonal variation in precipitation [12,13]. Patterns of endemism farther back into the Palaeozoic are presently unclear because the Lopingian was preceded by a poorly-understood period of taxonomic turnover during the Guadalupian [31]. Analysis of older Palaeozoic time bins will be required to elucidate changes in endemism during the earlier history of Pangaea.

232 This background trend of increasing endemism contrasts sharply with the increase in
233 pBC immediately following each mass extinction. This highlights the unique
234 macroevolutionary regimes associated with mass extinctions[24,32], with post-extinction
235 'disaster faunas' being the result of the abnormal selective conditions operating in the wake
236 of these crises. An increase in global cosmopolitanism, with a prevalence of 'disaster taxa',
237 has also been observed in marine invertebrates across the Ordovician-Silurian [33,34], Permian-
238 Triassic [35,36], and Cretaceous-Palaeogene [14] mass extinctions, although these studies have not
239 explicitly incorporated phylogenetic data. Similarly, more generalized insect-plant
240 associations show higher survivorship across the Cretaceous-Tertiary mass extinction[37] and,
241 on the smaller scale, Pleistocene-Holocene warming resulted in a greater unevenness of small
242 mammal faunas in northern California[38]. Our demonstration of a similar signal in terrestrial
243 communities in the latest Palaeozoic and early Mesozoic suggests that mass extinctions exert
244 predictable biogeographical influences. However, the Permian-Triassic and Triassic-Jurassic
245 events may be unique amongst terrestrial mass extinctions due to the presence of Pangaea,
246 where the perceived reduction in barriers to overland dispersal might have facilitated the
247 development of high levels of terrestrial cosmopolitanism. Extending the methodology
248 employed here to other extinction events, such as for terrestrial faunas across the Cretaceous–
249 Palaeogene boundary, will provide further tests of generalizable biogeographic trends across
250 different mass extinction events.

251 These common trends observed in the fossil record have the potential to inform
252 modern conservation efforts, given that the current biodiversity crisis is acknowledged as
253 representing another mass extinction event [39]. Global homogenisation due to human
254 activities, such as landscape simplification[40], ecosystem disruption[40–42], anthropogenic
255 climate change[4,38,42], and introduction of exotic species[42–44], represents a principal threat to
256 contemporary biodiversity[43,45]. Ongoing extinction will exacerbate this[42,43] with a shift

257 towards a more generalised ‘disaster’ fauna projected on the basis of current trends [4,46]. The
258 observation of global collapse in biogeographic structure accompanying previous mass
259 extinctions, as documented here, corroborates this and is of key importance in forecasting the
260 biological repercussions of the current biodiversity crisis.

261

262 **Methods**

263 **Phylogeny**. An informal supertree of 1046 early amniote species ranging from 315–170 Ma
264 was constructed from pre-existing phylogenies (Fig. 2a; see Supplementary Note 1,
265 Supplementary Data 1). We used an informal supertree approach rather than a formal
266 supertree in order to maximise taxonomic sampling, including species that have not been
267 included in quantitative phylogenetic analyses. In addition to the taxa included in the
268 biogeographic connectedness analyses, this sample included some stratigraphically older taxa
269 in order to more accurately date deeper nodes. In order to account for phylogenetic
270 uncertainty, 100 time-calibrated trees, with random resolution of polytomies, were produced
271 from this supertree utilizing the ‘timePaleoPhy’ function of the paleotree package [53] in R
272 (version 3.2.3; *34*). Trees were dated according to first occurrence dates, with a minimum
273 branch length of 1 Myr.

274

275 **Taxon occurrences and ages**. A global occurrence database of 891 terrestrial amniote
276 species was assembled, primarily from the Paleobiology Database [47], with the addition of
277 some occurrences from the literature (see Supplementary Note 2, Supplementary Data 2).
278 Taxa were dated at stage level. They were then placed in the following time bins for analysis:
279 Lopingian, Early Triassic (Induan and Olenekian), Anisian, Ladinian, early Late Triassic
280 (Carnian–early Norian), late Late Triassic (late Norian–Rhaetian), early Early Jurassic

(Hettangian, Sinemurian), and late Early Jurassic (Pliensbachian, Toarcian). The Late Triassic was not split into its constituent stages due to the disproportionately long Norian stage [48–51]: rock units from this epoch were instead assigned to either the early Norian or the late Norian (see Supplementary Tables S1, S2).

**Geographic areas**. In order to conduct network and many other palaeobiogeographic analyses it is necessary to identify a series of geographically discrete areas (the localities of the taxon-locality network in the network methodology). These areas are typically defined solely on the basis of geography (rather than shared flora or fauna) because the aim is to test faunal similarity between geographically distinct regions of the world. For example, previous analyses have commonly used modern continents as input areas[10, 11, 13, 15]. This traditional approach is potentially problematic on a supercontinent where, for example, eastern North American and north-western African localities were much closer to each other than to localities in southwestern North America or southern Africa. Instead, we defined our geographic areas on the basis of k-means clustering of palaeocoordinate data for 2144 terrestrial fossil occurrences from the relevant time span, obtained mostly from the Paleobiology Database (see Supplementary Note S3). Importantly, this approach does not require or use any information on taxonomy or phylogeny – it is solely designed to find geographically-discrete clusters of fossil localities – and thus it is fully independent from the subsequent network analyses.

Data were binned at epoch level, with each epoch analysed separately to avoid confusion arising from continental movements. K-means clustering was performed within R, varying the value of *k* from 5–15. For each value of *k,* the analysis was repeated with ten random starts, with 100 replicates). Performance of different analyses was then compared on

305 the basis of the percentage of variance explained, and results were compared with
306 palaeogeographic reconstructions through this interval [10,52] (Supplementary Table 3; full
307 results are given as Supplementary Data 3). This resulted in the designation of ten discrete
308 palaeogeographic regions that each represent localities for the network analyses (Fig. 1b).
309 Taxa were assigned to one or more regions as appropriate, yielding a taxon-locality matrix
310 for each time bin (Supplementary Data 4).

311

312

313 **Phylogenetic network biogeography analyses**. Non-phylogenetic biogeographic
314 connectedness (BC) was previously quantified [3] as the rescaled density of a taxon-locality
315 matrix, calculated as follows:

316 $$BC = \frac{O-N}{(L*N)-N} \quad [1]$$

317 In this formula, $O$ = the number of links in the network (the sum of all values in a taxon-
318 locality matrix, which will equal the number of occurrences in a non-phylogenetic analysis),
319 $N$ = the number of taxa, and $L$ = the number of localities. This gives the ratio between the
320 number of taxa present beyond a single locality and the maximum possible number of
321 occurrences (i.e., every taxon present at every locality). Aside from whether a taxon is
322 identical or not, no further phylogenetic information is included using this method – links are
323 only considered where an individual taxon is shared between different localities, and are all
324 equally weighted.

325 Herein, this method was modified to include phylogenetic information (phylogenetic
326 biogeographic connectedness = pBC) by weighting links between taxa as inversely
327 proportional to the phylogenetic distances between them. Phylogenetic distances between

328 taxa were measured by summing the branch lengths in millions of years representing the
329 shortest distance between two taxa. This was then scaled against the maximum possible
330 phylogenetic distance (i.e., the total distance of the summed branch lengths between the two
331 most distantly related taxa). This scaled value was then subtracted from one to yield the
332 weight of each link: the values of links between taxa hence vary between one (co-occurrence
333 of the same species in two separate localities) and zero (when comparing the two most
334 distantly related taxa in the taxon-locality matrix). The sum of the reweighted taxon-locality
335 matrix was then substituted for *O* in equation 1 to yield a value of phylogenetic
336 biogeographic connectedness. This method has been made available as the "BC" function
337 within the R package dispeRse [55] (available at github.com/laurasoul/dispeRse): example
338 analysis scripts are given as Supplementary Data 5 and Supplementary Data 6. It should be
339 noted that a given value of pBC will be a non-unique solution: the same value could
340 theoretically be generated by many links between distantly-related taxa or by fewer links
341 between more closely-related species. Disentangling these possibilities is difficult. However,
342 comparison of results with measured phylogenetic distances and number of taxa in each time
343 bin indicates that pBC results are not merely driven by differences in the relatedness of
344 sampled taxa, and instead reflect genuine biogeographical signal (see supplementary
345 information).

346 Analysis of a simulated null (stochastically generated) dataset indicated a predictable
347 and systematic pattern of increasing pBC through time. This is due to the increasing distance
348 from a persistent root to the tips through time, resulting in phylogenetic branch lengths
349 between nearest relative terminal taxa becoming proportionately shorter. In order to compare
350 pBC between different time bins, it is therefore necessary to remove this tendency for pBC to
351 increase in later time bins. We achieved this through the introduction of a constant, $\mu$, which
352 collapses all branches below a fixed "depth" such that root age is equal to $\mu$ million years

353 before the tips. The introduction of this constant also alleviates problems of temporal
354 superimposition of biogeographic signals that may otherwise occur. It means that pBC results
355 reported for each time bin reflect patterns generated by biogeographic processes in the
356 preceding $\mu$ million years, preventing these recent biogeographic signals of interest from
357 being swamped by those from deeper time intervals. A $\mu$ value of 15 was chosen based on the
358 results of sensitivity analyses varying the value of $\mu$ from 5–25 Myr in 1 Myr increments (see
359 Supplementary Note 7, Supplementary Fig 7).

360 This method was applied to the taxon-region matrix for each time bin, and the 100
361 time-calibrated supertrees, pruning taxa not present within the bin of interest (effectively
362 making each tree ultrametric) to calculate pBC. Jackknifing, with 10,000 replicates, was used
363 to calculate 95% confidence intervals. This analysis was then repeated without phylogenetic
364 information to gauge the importance of phylogeny on observed patterns.

365

366 **Taxon subset analyses.** In order to investigate the processes giving rise to observed changes
367 in cosmopolitanism over mass extinction events, analyses were also performed on two
368 taxonomic subsets. The first reanalysed time bins either side of each mass extinction (the
369 Lopingian and Early Triassic and late Late Triassic and early Early Jurassic) including only
370 small clades exhibiting high survivorship (<20 species, with ≥20% of lineages crossing the
371 extinction boundary). This was intended to minimize the influence of possible preferential
372 extinction of geographically-restricted taxa.

373 The removal of taxa during mass extinctions opens new vacancies in ecospace,
374 promoting adaptive radiations in surviving, often previously marginal, clades [56,57]. For
375 example, the Permian-Triassic mass extinction is seen as a causal factor in the succeeding
376 radiation of epicynodonts [58] and archosaurs [3,59,60], and the Triassic—Jurassic radiation as

377 pivotal in the diversification of crocodylomorph[61] and dinosaur clades [20,62]. 'Disaster faunas'
378 will hence be expected to be composed of relatively recently diverging clades, as surviving
379 taxa diversify into broader geographic ranges (e.g., [59]). To test the significance of this, we
380 reanalysed the time bins immediately following each mass extinction, including only clades
381 that branched <2 Myr prior to or after the boundary. In order to ensure that the results of this
382 analysis reflected differences in the post-extinction bins as opposed to an artefact of clade
383 age, also performed analyses applying this filter to the other time bins (see Supplementary
384 Note 6).

385

386 **Geographically localised analyses.** To atomise global pBC signals into hemispheric trends,
387 pBC was re-calculated for Laurasian and Gondwanan areas separately following an identical
388 procedure to that for global analyses. Finally, to compare global results obtained from this
389 new method with the more localised analysis of Sidor *et al.* [3], another set of analyses was
390 performed following the taxonomic sampling of the latter. Terrestrial amniote occurrences
391 from the late Permian and Middle Triassic of the Karoo Basin of South Africa; Luangwa
392 Basin of Zambia; Chiweta beds of Malawi; Ruhuhu Basin of Tanzania, and the Beacon Basin
393 of Antarctica were taken from the dataset of Sidor *et al.* [3]. These data and the 100 time-
394 calibrated trees described above were then used to calculate BC and pBC between these
395 basins for each of the sampled time bins.

396

397 **References**


398 1. Erwin, D. H. Lessons from the past: biotic recoveries from mass extinctions. *Proc.*
399 *Natl. Acad. Sci. U. S. A.* **98,** 5399–5403 (2001).

400 2. Sahney, S. & Benton, M. J. Recovery from the most profound mass extinction of all

time. *Proc. R. Soc. B Biol. Sci.* **275,** 759–65 (2008).

3. Sidor, C. A. *et al.* Provincialization of terrestrial faunas following the end-Permian mass extinction. *Proc. Natl. Acad. Sci. U. S. A.* **110,** 8129–33 (2013).

4. Blois, J. L., Zarnetzke, P. L., Fitzpatrick, M. C. & Finnegan, S. Climate change and the past, present, and future of biotic interactions. *Science* **341,** 499–504 (2013).

5. Raup, D. M. Size of the Permo-Triassic bottleneck and its evolutionary implications. *Science* **206,** 217–218 (1979).

6. Chen, Z.-Q. & Benton, M. J. The timing and pattern of biotic recovery following the end-Permian mass extinction. *Nat. Geosci.* **5,** 375–383 (2012).

7. Roopnarine, P. D., Angielczyk, K. D., Wang, S. C. & Hertog, R. Trophic network models explain instability of Early Triassic terrestrial communities. *Proc. R. Soc. B Biol. Sci.* **274,** 2077–86 (2007).

8. Payne, J. L. *et al.* Early and Middle Triassic trends in diversity, evenness, and size of foraminifers on a carbonate platform in south China: Implications for tempo and mode of biotic recovery from the end-Permian mass extinction. *Paleobiology* **37,** 409–425 (2011).

9. Fraser, N. C. & Sues, H.-D. The beginning of the 'Age of Dinosaurs': A brief overview of terrestrial biotic changes during the Triassic. *Earth Environ. Sci. Trans. R. Soc. Edinburgh* **101,** 189–200 (2010).

10. Scotese, C. R. A continental drift flipbook. *J. Geol.* **11,** 729–741 (2004).

11. Ezcurra, M. D. Biogeography of Triassic tetrapods: Evidence for provincialism and driven sympatric cladogenesis in the early evolution of modern tetrapod lineages. *Proc. Biol. Sci.* **277,** 2547–2552 (2010).

12. Whiteside, J. H., Grogan, D. S., Olsen, P. E. & Kent, D. V. Climatically driven biogeographic provinces of Late Triassic tropical Pangea. *Proc. Natl. Acad. Sci. U. S. A.* **108,** 8972–8977 (2011).

13. Whiteside, J. H. *et al.* Extreme ecosystem instability suppressed tropical dinosaur dominance for 30 million years. *Proc. Natl. Acad. Sci.* **112,** 7909–7913 (2015).

14. Jablonski, D. & Raup, D. M. Selectivity of end-Cretaceous marine bivalve extinctions. *Science* **268,** 389–391 (1995).

15. Raup, D. M. & Jablonski, D. Geography of end-Cretaceous marine bivalve extinctions. *Science* **260,** 971–973 (1995).

16. Jablonski, D. Geographic variation in the molluscan recovery from the end-Cretaceous Extinction. *Science* **279,** 1327–1330 (1998).

17. Vilhena, D. a *et al.* Bivalve network reveals latitudinal selectivity gradient at the end-Cretaceous mass extinction. *Sci. Rep.* **3,** 1790 (2013).

18. Sues, H.-D. & Fraser, N. C. *Triassic life on land: The great transition*. (Columbia University Press, 2010).

19. Dunhill, A. M. & Wills, M. A. Geographic range did not confer resilience to extinction in terrestrial vertebrates at the end-Triassic crisis. *Nat. Commun.* **6,** 7980 (2015).

20. Brusatte, S. L., Benton, M. J., Ruta, M. & Lloyd, G. T. Superiority, competition, and opportunism in the evolutionary radiation of dinosaurs. *Science* **321,** 1485–1488 (2008).

21. Luo, Z.-X. Transformation and diversification in early mammal evolution. *Nature* **450,** 1011–1019 (2007).

22. Gould, S. J. The paradox of the first tier: An agenda for paleobiology. *Paleobiology* **11,** 2–12 (1985).

23. Gould, S. J. *Wonderful Life*. (W. W. Norton, 1989).

24. Jablonski, D. Mass extinctions and macroevolution. *Paleobiology* **31,** 192–210 (2005).

25. Novas, F. E., Ezcurra, M. D., Chatterjee, S. & Kutty, T. S. New dinosaur species from the Upper Triassic Upper Maleri and Lower Dharmaram formations of Central India. *Earth Environ. Sci. Trans. R. Soc. Edinburgh* **101,** 333–349 (2010).

26. Bernardes-de-Oliveira, M. E. *et al.* Mesophytic gondwanan paleofloras from Brazil and India: Composition and paleoclimatical approach. *Paleontol. Cenários Vida* **4,** 93–105 (2011).

27. Césari, S. N. & Colombi, C. E. A new Late Triasssic phytogeographical scenario in westernmost Gondwana. *Nat. Commun.* **4,** 1889 (2013).

28. Sellwood, B. W. & Valdes, P. J. Mesozoic climates: General circulation models and the rock record. *Sediment. Geol.* **190,** 269–287 (2006).

29. Shubin, N. H. & Sues, H.-D. Biogeography of early Mesozoic continental tetrapods: Patterns and implications. *Paleobiology* **17,** 214–230 (1991).

30. Golonka, J. Late Triassic and Early Jurassic palaeogeography of the world. *Palaeogeogr. Palaeoclimatol. Palaeoecol.* **244,** 297–307 (2007).

31. Bambach, R. K. Phanerozoic Biodiversity Mass Extinctions. *Annu. Rev. Earth Planet. Sci.* **34,** 127–155 (2006).

32. Jablonski, D. Background and mass extinctions The alternation of macroevolutionary regimes. *Science* **231,** 129–133 (1986).

468 33. Brenchley, P. J., Marshall, J. D. & Underwood, C. J. Do all mass extinctions represent
469 an ecological crisis? Evidence from the Late Ordovician. *Geol. J.* **36,** 329–340 (2001).

470 34. Sheehan, P. M. The Late Ordovician Mass Extinction Event. *Annu. Rev. Earth Planet.*
471 *Sci.* **29,** 331–364 (2001).

472 35. Schubert, J. K. & Bottjer, D. J. Aftermath of the Permian-Triassic mass extinction
473 event: Paleoecology of Lower Triassic carbonates in the western USA. *Palaeogeogr.*
474 *Palaeoclimatol. Palaeoecol.* **116,** 1–39 (1995).

475 36. Rodland, D. L. & Bottjer, D. J. Biotic recovery from the end-Permian mass extinction;
476 Behavior of the inarticulate brachiopod *Lingula* as a disaster taxon. *Palaios* **16,** 95–101
477 (2001).

478 37. Labandeira, C. C., Johnson, K. R. & Wilf, P. Impact of the terminal Cretaceous event
479 on plant-insect associations. *Proc. Natl. Acad. Sci. U. S. A.* **99,** 2061–2066 (2002).

480 38. Blois, J. L., McGuire, J. L. & Hadly, E. A. Small mammal diversity loss in response to
481 late-Pleistocene climatic change. *Nature* **465,** 771–774 (2010).

482 39. Barnosky, A. D. *et al.* Has the Earth's sixth mass extinction already arrived? *Nature*
483 **471,** 51–57 (2011).

484 40. Western, D. Human-modified ecosystems and future evolution. *Proc. Natl. Acad. Sci.*
485 *U. S. A.* **98,** 5458–5465 (2001).

486 41. Vitousek, P. M., Mooney, H.A, Lubchenco, J. & Melillo, J. M. Human domination of
487 Earth's ecosystems. *Science* **277,** 494–499 (1997).

488 42. McKinney, M. L. & Lockwood, J. L. Biotic homogenization: A few winners replacing
489 many losers in the next mass extinction. *Trends Ecol. Evol.* **14,** 450–453 (1999).

490 43. Olden, J. D., Poff, N. L., Douglas, M. R., Douglas, M. E. & Fausch, K. D. Ecological
491 and evolutionary consequences of biotic homogenization. *Trends Ecol. Evol.* **19,** 18–
492 24 (2004).

493 44. Sax, D. F. & Gaines, S. D. Species invasions and extinction: the future of native
494 biodiversity on islands. *Proc. Natl. Acad. Sci.* **105,** 11490–11497 (2008).

495 45. Pereira, H. M. *et al.* Scenarios for global biodiversity in the 21st century. *Science* **330,**
496 1496–1501 (2010).

497 46. Jackson, J. B. C. Colloquium paper: Ecological extinction and evolution in the brave
498 new ocean. *Proc. Natl. Acad. Sci. U. S. A.* **105,** 11458–11465 (2008).

499 47. M. Carrano, R. J. Butler, R. Benson, T. Liebrecht *et al*. (2016) Taxonomic occurrences
500 of Lopingian to Toarcian recorded in the *Paleobiology Database*.
501 https://paleobiodb.org.

502 48. Muttoni, G. *et al.* Tethyan magnetostratigraphy from Pizzi Mondello (Sicily) and
503 correlation to the Late Triassic Newark astrochronological polarity time scale Tethyan
504 magnetostratigraphy from Pizzo Mondello (Sicily) and correlation to the Late Triassic
505 Newark astrochron. *Geol. Soc. Am. Bull.* **116,** 1043–1058 (2004).

506 49. Irmis, R. B., Martz, J. W., Parker, W. G. & Nesbitt, S. J. Re-evaluating the correlation
507 between Late Triassic terrestrial vertebrate biostratigraphy and the GSSP-defined
508 marine stages. *Albertiana* **38,** 40–52 (2009).

509 50. Olsen, P. E., Kent, D. V & Whiteside, J. H. Implications of the Newark Supergroup-
510 based astrochronology and geomagnetic polarity time scale ( Newark-APTS ) for the
511 tempo and mode of the early diversi fi cation of the Dinosauria. **2011,** 201–229 (2011).

512 51. Kent, D. V., Malnis, P. S., Colombi, C. E., Alcober, O. A. & Martinez, R. N. Age

513 constraints on the dispersal of dinosaurs in the Late Triassic from magnetochronology
514 of the Los Colorados Formation (Argentina). *Proc. Natl. Acad. Sci.* **111,** 7958–7963
515 (2014).

516 52. Scotese, C. R. Atlas of Earth history. *PALEOMAP Proj. Arlingt. Dept. Geol. Univ.*
517 *Texas Arlingt.* **1,** (2001).

518 53. Bapst, D. W. Paleotree: An R package for paleontological and phylogenetic analyses
519 of evolution. *Methods Ecol. Evol.* **3,** 803–807 (2012).

520 54. Team, R. development core. R: A language and environment for statistical computing.
521 *R Found. Stat. Comput. Vienna, Austria.* **ISBN 3-900,** (2008).

522 55. Soul, L. C. & Lloyd, G. T. dispeRse: Models For Paleobiogeography. Available at:
523 https://github.com/laurasoul/dispeRse

524 56. Schluter, D. *The ecology of adaptive radiation*. (Oxford University Press, 2000).

525 57. Yoder, J. B. *et al.* Ecological opportunity and the origin of adaptive radiations. *J. Evol.*
526 *Biol.* **23,** 1581–1596 (2010).

527 58. Ruta, M., Botha-Brink, J., Mitchell, S. a & Benton, M. J. The radiation of cynodonts
528 and the ground plan of mammalian morphological diversity. *Proc. Biol. Sci.* **280,**
529 20131865 (2013).

530 59. Butler, R. J. *et al.* The sail-backed reptile Ctenosauriscus from the latest Early Triassic
531 of Germany and the timing and biogeography of the early archosaur radiation. *PLoS*
532 *One* **6,** (2011).

533 60. Pinheiro, F. L., França, M. A. G., Lacerda, M. B., Butler, R. J. & Schultz, C. L. An
534 exceptional fossil skull from South America and the origins of the archosauriform
535 radiation. *Sci. Rep.* **6,** 22817 (2016).

536 61. Toljagic, O. & Butler, R. J. Triassic-Jurassic mass extinction as trigger for the
537 Mesozoic radiation of crocodylomorphs. *Biol. Lett.* **9,** 1–4 (2013).

538 62. Benton, M. J., Forth, J. & Langer, M. C. Models for the rise of the dinosaurs. *Curr.*
539 *Biol.* **24,** R87–R95 (2014).

540 63. Rothkugel, S. & Varela, S. paleoMap: Spatial Paleobiodiversity Combined with
541 Paleogeography. (2015). Available at: https://github.com/NonaR/paleoMap

542 **Acknowledgments**

543 We thank R. Benson, R. Close, D. Cashmore, and E. Dunne for discussion. This research
544 received funding from the Marie Curie Actions (grant 630123 to RJB), an ERC Starting
545 Grant (grant 637483 to RJB), and a Discovery Early Career Researcher Award (grant
546 DE140101879 to GTL). This is Paleobiology Database official publication 289.

547 **Author contributions:** G.T.L., R.J.B. and M.D.E conceived the research. G.T.L. and R.J.B.
548 wrote new functions as required for these analyses. D.J.B. compiled the data, performed the
549 analyses and prepared the figures. All authors discussed results and contributed to writing the
550 manuscript.

551 **Data availability:** All data analysed in this study and example code are available in the
552 supplementary data file**s.**

553 **Competing financial interests:** The authors declare no competing financial interests.

## Figure legends

**Fig. 1: Schematic illustration of network biogeography methods.** a) Simplified phylogeny of Dicynodontia. b-c) Taxon-locality networks. Localities are indicated by the large, pale brown circles, taxa are coloured as in a). Taxa are connected by brown lines to the locality at which they occur. b) Rescaled non-phylogenetic biogeographic connectedness (BC) of Sidor *et al*. [3]. A single taxon, *Kannemeyeria* (yellow), is present at all three localities, resulting in a link of value=1 (solid black line) between each locality. c) Phylogenetic biogeographic connectedness (pBC), as proposed here. Links (grey lines) between taxa from different localities are weighted inversely to their phylogenetic relatedness. Line thickness and shade is proportional to the strength of the link (and thus inversely proportional to phylogenetic distance between the two taxa).

**Fig. 2: Phylogenetic framework and biogeographic regions employed in this study.** a) Informal supertree of amniotes used in the analyse. b) Triassic palaeogeography, redrawn after [10,30,63], with the geographic regions used as localities for the network analysis. 1: Western USA, British Columbia, Mexico, Venezuela; 2: Eastern USA, Eastern Canada, Morocco, Algeria; 3: Europe, Greenland; 4: Russia; 5: China, Thailand, Kyrgyzstan; 6: Argentina; 7: Brazil, Uruguay, Namibia; 8: South Africa, Lesotho, Zimbabwe; 9: Tanzania, Zambia, Madagascar, India, Israel, Saudi Arabia; 10: Antarctica, southeast Australia.

**Fig. 3: Results from BC analysis of Lopingian-Early Jurassic terrestrial amniotes.** Results from both non-phylogenetic (BC, red) and phylogenetic (pBC, blue) analyses of global biogeographic connectedness are shown. Shaded polygons represent ninety-five percent confidence intervals (calculated from jackknifing with 10,000 replicates) for both the BC and pBC analyses. The Permian-Triassic boundary (PTB) and Triassic-Jurassic boundary (TJB) extinction events are indicated by dotted lines. E. Tr. refers to the Early Triassic.

578 **Fig. 4: Results from BC analysis of taxonomic subsets.** Comparison of results for data
579 subsets across the Permian-Triassic (a) and Triassic-Jurassic (b) mass extinctions. Results for
580 the entire dataset are in black, those for less inclusive clades showing high survivorship in
581 red, and those for the most recently diverging taxa in purple. Ninety-five percent confidence
582 intervals, calculated from jackknifing with 10,000 replicates, are indicated.

583 **Fig. 5: Results from BC analysis of geographically localised areas.** a) Comparison of pBC
584 trends during the Lopingian-Early Jurassic from Gondwana localities (in green) against those
585 for Laurasia (in purple). Ninety-five percent confidence intervals are indicated. Abbreviations
586 as in Fig. 3; E. Jur. refers to Early Jurassic. Ninety-five percent confidence intervals,
587 calculated from jackknifing with 10,000 replicates, are indicated. b) Results from analysis of
588 basin-level terrestrial amniote occurrences from the late Permian and Middle Triassic of
589 southern Pangaea, from the dataset of Sidor *et al*. [3]. Phylogenetic BC results are given in
590 blue, non-phylogenetic BC in red. Ninety-five percent confidence intervals, calculated from
591 jackknifing with 1000 replicates, are indicated.

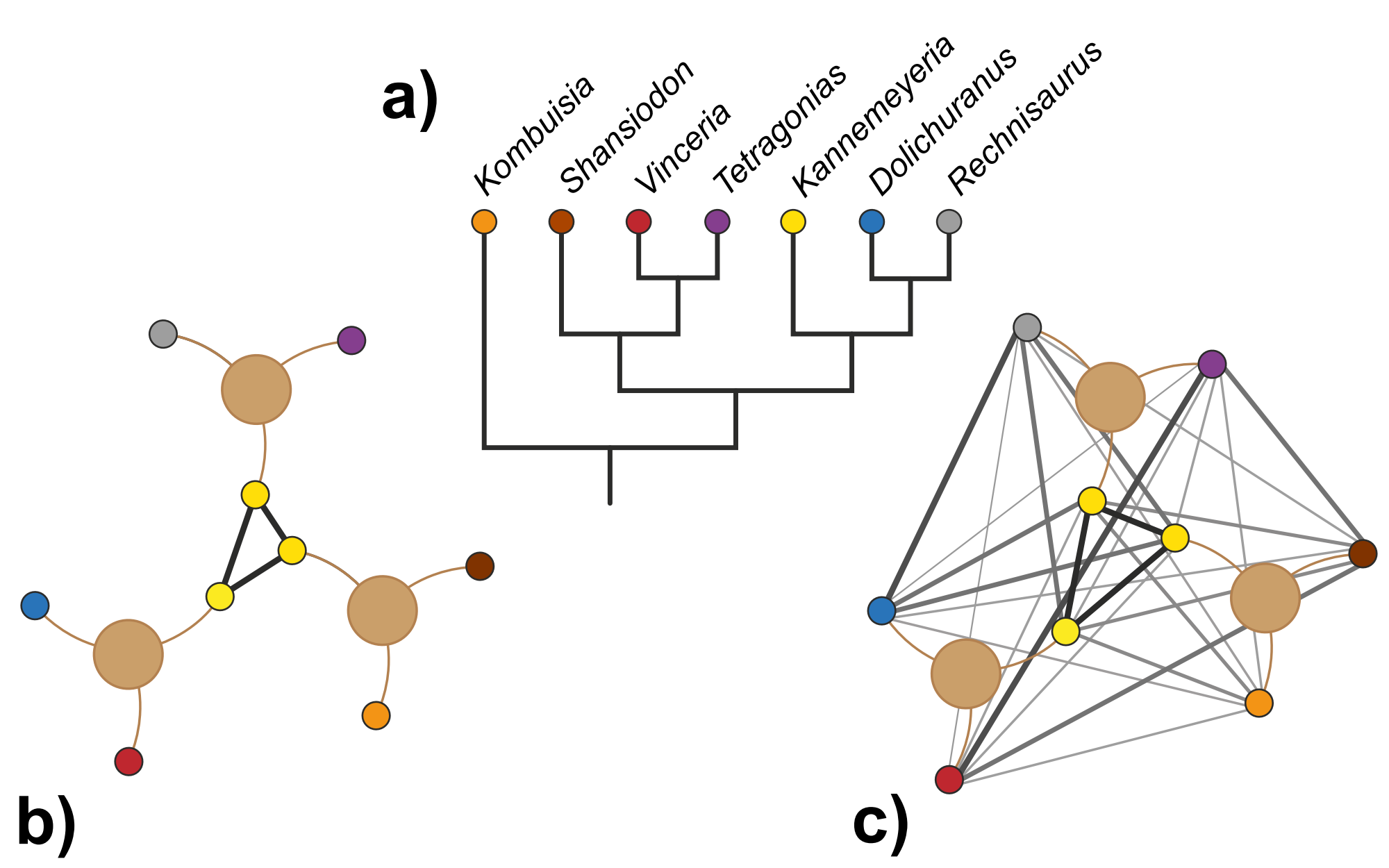
a)
Kombuisia
Shansiodon
Vinceria
Tetragonias
Kannemeyeria
Dolichuranus
Rechnisaurus
b)
c)

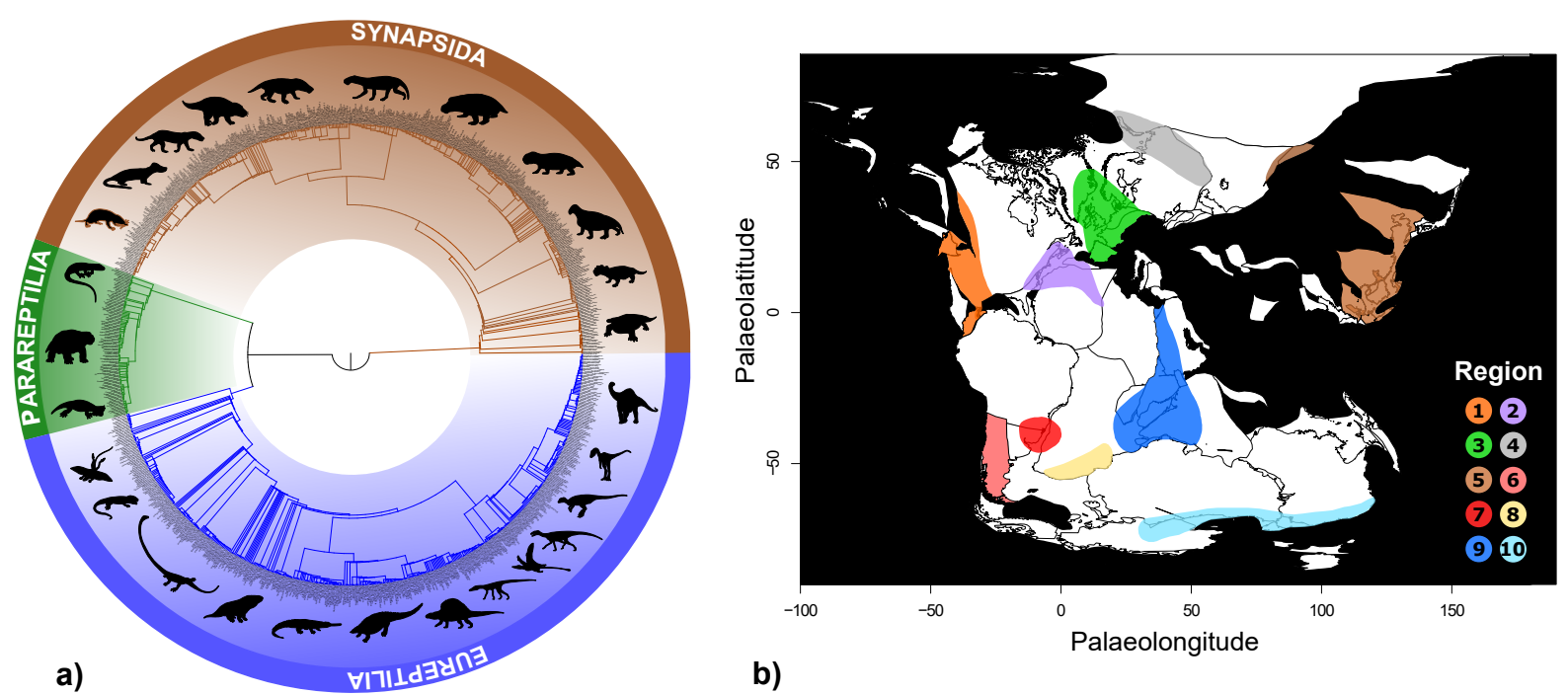
SYNAPSIDA
PARAREPTILIA
EUREPTILIA
a)
Palaeolatitude
50
0
−50
−100
−50
0
50
100
150
Palaeolongitude
Region
1
2
3
4
5
6
7
8
9
10
b)

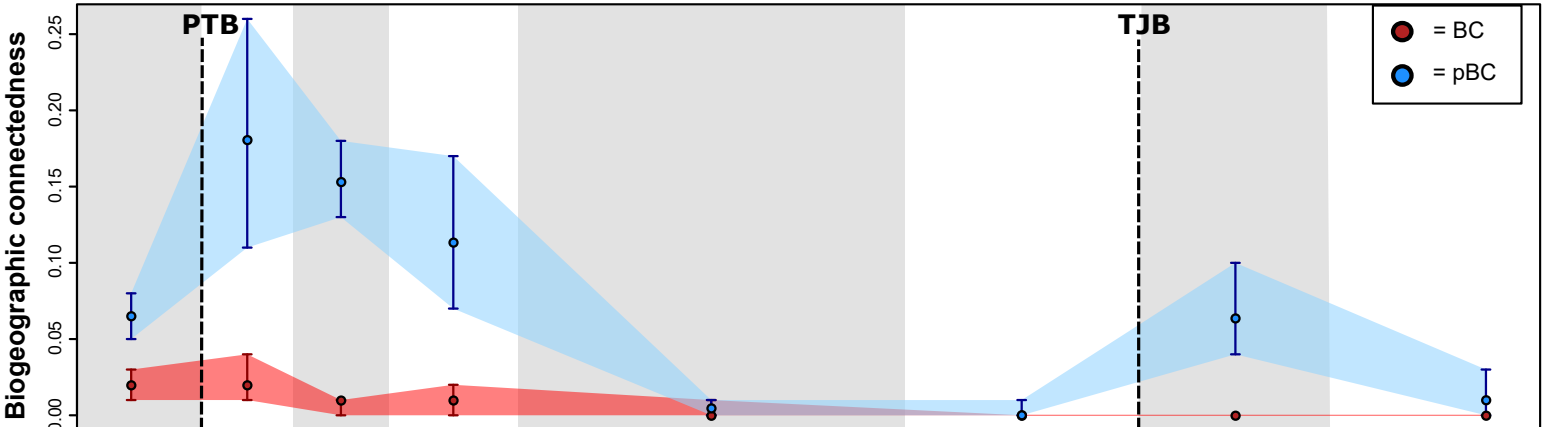
Biogeographic connectedness
0.00
0.05
0.10
0.15
0.20
0.25
PTB
TJB
= BC
= pBC
Lopingian
E. Tr.
Anisian
Ladinian
early Late Triassic
late Late Triassic
early Early Jurassic
late Early Jurassic

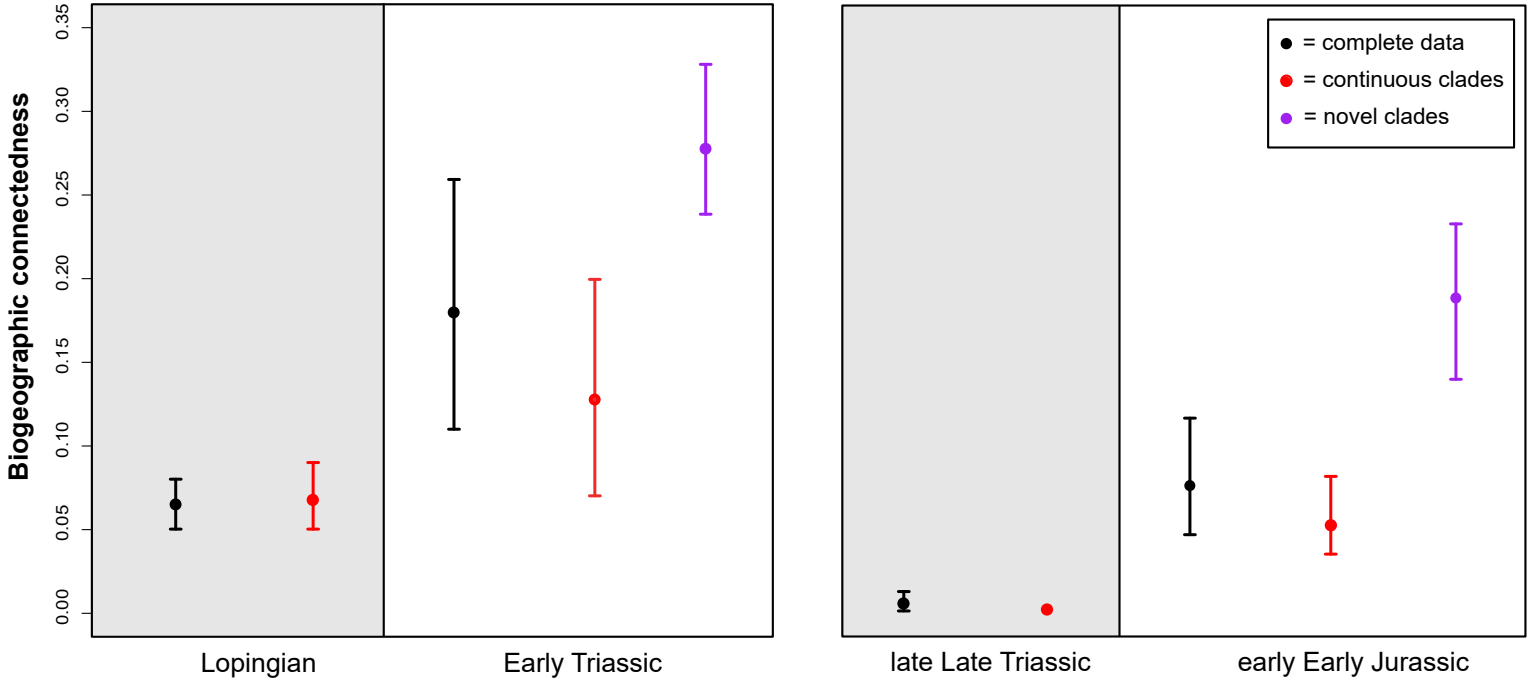
Biogeographic connectedness
0.00
0.05
0.10
0.15
0.20
0.25
0.30
0.35
= complete data
= continuous clades
= novel clades
Lopingian
Early Triassic
late Late Triassic
early Early Jurassic

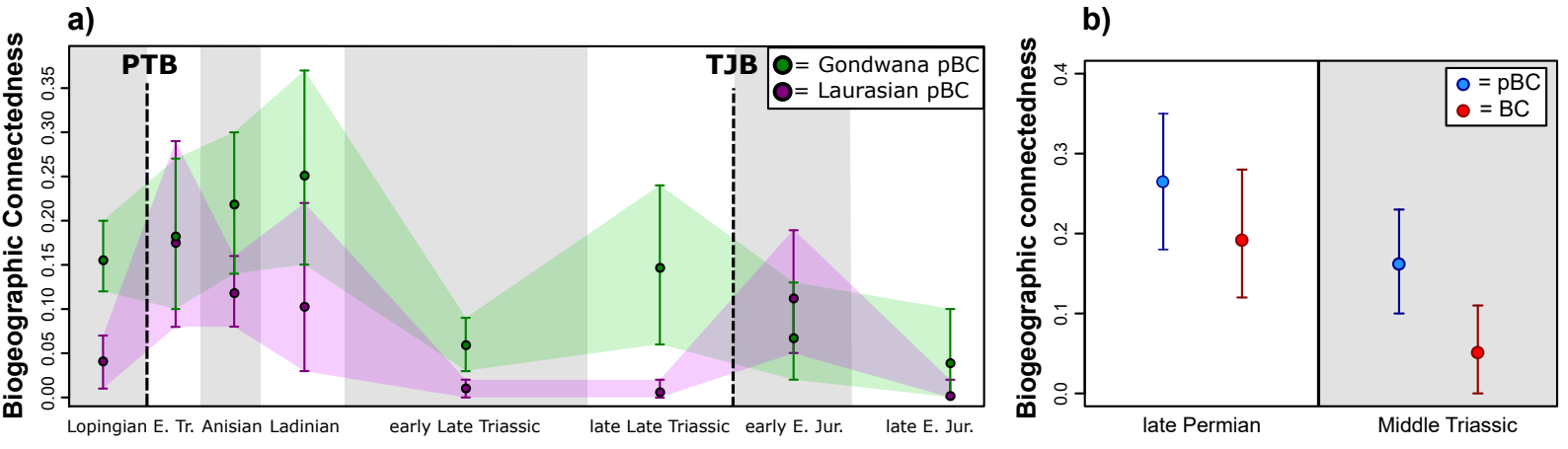
a)
PTB
TJB
= Gondwana pBC
= Laurasian pBC
Biogeographic Connectedness
0.00
0.05
0.10
0.15
0.20
0.25
0.30
0.35
Lopingian
E. Tr.
Anisian
Ladinian
early Late Triassic
late Late Triassic
early E. Jur.
late E. Jur.
b)
= pBC
= BC
Biogeographic connectedness
0.0
0.1
0.2
0.3
0.4
late Permian
Middle Triassic